Letter

Direct measurement of spin-flip rates of a self-assembled InAs double quantum dot in single-electron tunneling

Olfa Dani,[1] Robert Hussein,[2] Johannes C. Bayer,[1] Klaus Pierz,[3] Sigmund Kohler,[4] and Rolf J. Haug[1]
[1]*Institut für Festkörperphysik, Leibniz Universität Hannover, D-30167 Hanover, Germany*
[2]*Institut für Festkörpertheorie und -optik, Friedrich-Schiller-Universität Jena, D-07743 Jena, Germany*
[3]*Physikalisch-Technische Bundesanstalt, Bundesallee 100, D-38116 Braunschweig, Germany*
[4]*Instituto de Ciencia de Materiales de Madrid, CSIC, E-28049 Madrid, Spain*

(Received 18 October 2023; accepted 29 February 2024; published 15 March 2024)

Spin flips are one of the limiting factors for spin-based information processing. We demonstrate a transport approach for determining the spin-flip rates of a self-assembled InAs double quantum dot occupied by a single electron. In such devices, different Landé factors lead to an inhomogeneous Zeeman splitting, so that the two spin channels can never be at resonance simultaneously, leading to a spin blockade at low temperatures. This blockade is analyzed in terms of spin flips for different temperatures and magnetic fields. Our results are in good agreement with a quantum master equation that combines the dot-lead couplings with ohmic dissipation stemming from spin-flip cotunneling.

DOI: 10.1103/PhysRevB.109.L121404

Introduction. Quantum computing based on spins in coupled quantum dots (QDs) was proposed 25 years ago [1] and appears to be within reach nowadays [2–4]. Initialization and control of the spin is critically dependent on spin coherence. A number of theoretical works showed its sensitive dependence on hyperfine coupling [5] or cotunneling [6,7], as well as on the influence of Markovian [8] or non-Markovian [9] noise. The spin-phonon coupling mediated by a spin-orbit interaction [10,11] is often quite small, and the dominating spin decoherence is generally assumed to happen via a hyperfine interaction. Spin relaxation rates were addressed experimentally for single QDs [12–17] and also for coupled QDs [18–23]. There the decay rate as a function of the Zeeman splitting hints at the dominating dissipation process. Spin coherence in coupled QDs was mostly studied in the context of the spin blockade [18] based on the energetic difference between singlet and triplet two-electron states. These two-electron states relax the spin predominantly via a hyperfine interaction and a spin-orbit interaction in III-V semiconductors [11,24,25], whereas in silicon and germanium QDs also cotunneling [26–30] can be of importance. For transport phenomena that depend on the dynamics of a single spin in a double quantum dot (DQD), only very few studies exist [23,31,32].

Here, we demonstrate how to directly extract the spin-flip rate for a single spin in coupled QDs from the single-electron tunneling current. We use a DQD with a Zeeman level structure similar to the one of Ref. [31], but with an interdot tunneling much smaller than the typical detuning. Then, by contrast, the resulting current blockade is resolved by spin flips. For their theoretical description, we consider spin-flip cotunneling [6,7], i.e., dissipative spin transitions accompanied by excitations at the Fermi surface of a lead. As a consequence, the spin experiences ohmic dissipation [33,34], which fits the experimental data rather well, i.e., we show that spin-flip cotunneling is the dominant mechanism for spin relaxation in our DQD occupied by a single electron.

Experiment. We use vertically coupled self-assembled InAs QDs embedded in a GaAs-AlAs heterostructure. Due to the lattice mismatch of InAs and AlAs, pyramid-shaped QDs are formed and vertically aligned [35]. The dot in the second layer is slightly larger than the QD in the first one [36] due to the change in strain field. The diameter of such QDs typically is 10–20 nm and their height is between 2 and 4 nm. In these small QDs the strong confinement leads to the Landé g factor deviating strongly from the bulk value, approaching $g = 2$ of the free electron with decreasing dot sizes. The effective thickness of the middle and top barriers is reduced by the QDs partially penetrating the AlAs layers, which results in asymmetric dot-lead tunneling rates. The device sketched in Fig. 1(c) is similar to the ones used in Refs. [32,37,38]. For zero bias, the QD levels are above the Fermi energy and tunneling is not possible, whereas for finite bias voltage the QD levels are shifted by the electric field and brought into resonance and into the transport window.

The color graphs in Figs. 1(a) and 1(b) show the measured current through the DQD as a function of bias voltage V and magnetic field up to $B = 1$ T at temperatures $T = 1.5$ K and $T = 100$ mK, respectively. The magnetic field was applied perpendicular to the current (parallel to the layer structure). The graphs for $B = 0$ show a peak at $V \approx 138.25$ mV $\equiv V_0$, owing to the resonant tunneling of single electrons through the InAs DQD. The resonance originates from tunnel cycles with the occupation $(0, 0) \to (1, 0) \to (0, 1)$, where only a single electron is present in the DQD. At $T = 1.5$ K, for increasing magnetic field the single resonance splits into two peaks (peak I on the left and peak II on the right). At $T = 100$ mK [Fig. 1(b)], the resonant tunneling peak amplitude at $B = 0$ is higher [32] and decreases drastically already with small magnetic fields ∼0.25 T applied. The amplitude of peak I

 ©2024 American Physical Society

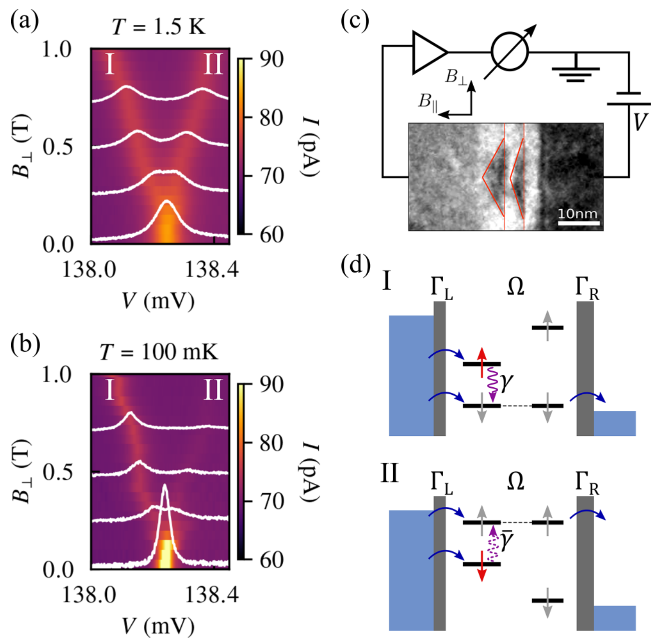

FIG. 1. (a) Current-voltage characteristic of InAs DQDs as a function of the magnetic field perpendicular to the tunneling current at $T = 1.5$ K, showing a current peak at $V \approx 138.25$ mV for $B = 0$. The white lines depict cuts along the color graphs. (b) The same for $T = 100$ mK. (c) Transmission electron microscopy (TEM) image of an InAs DQD shown in a schematic picture of the setup and the different magnetic field directions used. (d) Sketch of the transport channels for the different situations of resonance I and II. Due to the inhomogeneous Zeeman splittings always one channel is off resonant. An electron may be trapped in that channel and block transport until a spin flip (purple arrow) brings the electron to the resonant channel.

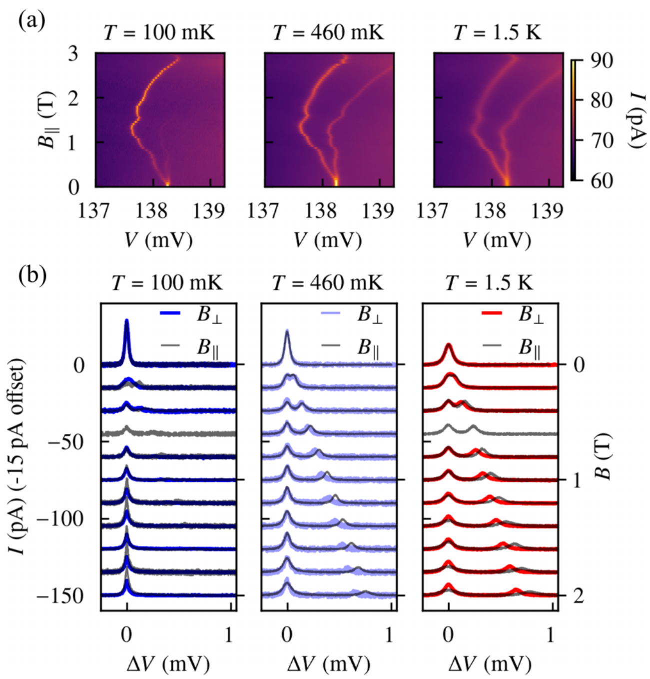

FIG. 2. (a) Magnetic field dependence of the tunneling current as function of voltage for magnetic field applied parallel to the tunneling current for three different temperatures $T = 100$ mK, 460 mK, and 1.5 K. (b) Tunneling current as a function of applied voltage normalized to the position of resonance I for the two different magnetic field directions. Traces offset by -15 pA are shown for magnetic fields ranging from 0 up to 2 T in step sizes of 0.2 T.

stays at a low but finite level with increasing magnetic field, meanwhile the right peak fades away totally.

This asymmetry can be explained by the different effect of spin relaxation as sketched in Fig. 1(d). Due to the different sizes of the two dots, their g factors g_L and g_R are different and therefore the Zeeman splitting becomes inhomogeneous [39,40]. For $V < V_0$ (peak I) the spin-down Zeeman levels of both QDs are in resonance, such that we expect to find a current peak. An electron with spin up, however, entering the left dot will get stuck, because the right dot is off resonance, such that the resonant channel becomes blocked. This blockade can be resolved by a spin flip for all temperatures because it does not require a spin excitation. For $V > V_0$ (peak II) the spin-up Zeeman levels are in resonance and can generate a tunneling current. If a spin-down electron enters the left QD, it blocks the single-electron tunneling current. This blockade can be lifted by a spin flip to the spin-up level. However, its lifting requires spin excitation and thus is observed only at sufficiently high temperatures such that kT exceeds the Zeeman splitting. Therefore, we observe peak II at 1.5 K, but not at 100 mK for magnetic fields larger than 0.5 T.

It is worth emphasizing the difference to Ref. [31] where a similar level structure has been studied. There, the interdot tunneling Ω is two orders of magnitude larger, comes close to the Zeeman splittings, and exceeds the dot-lead couplings (in our setup by contrast, $\Omega \ll \Gamma_{L,R}$). Then the spin-up as well as the spin-down states hybridize and form delocalized orbitals. When all levels are within the voltage window, this causes a current peak at $V = V_0$ even in the absence of spin flips. By contrast, when Ω is much smaller than the difference of the Zeeman splittings, we observe a blockade which is resolved by spin flips. Hence the current peaks provide information on the spin-flip rates.

Figure 2(a) shows the current for various temperatures as a function of the bias voltage and the magnetic field $B_\parallel$ applied parallel to the current (perpendicular to the layer structure). The observed oscillations and shifts with the magnetic field originate from the Landau-level structure in the emitter. Nevertheless, the peak-to-peak distances of the double peak increase more or less linearly with the magnetic field as shown in Fig. 2(b), where the position of peak II is shown relative to the position of peak I. In the same way in Fig. 2(b) also the results for the other magnetic field direction are shown. In both cases, the observed difference in peak positions is given by $\Delta V = |g_L - g_R|\mu_B B/\eta$, with the gyromagnetic ratio g_ℓ of QD $\ell = L, R$ and the leverage factor η. The individual Zeeman splittings of the dots do not appear, only $\Delta g = g_L - g_R$ plays a role here. Taking into account the leverage factor of $\eta = 0.15$ we obtain for $B_\perp$ a difference $\Delta g = 0.85$, whereas for $B_\parallel$ the value is $\Delta g = 1$. Anisotropy of the g factor is well known for single InAs QDs [40–43] and can explain the dependence of Δg on the magnetic field direction.

Double quantum dot–environment model. For a theoretical description of our observations, we start with the model used in Ref. [32] and also consider spin-flip cotunneling [6,7]. In doing so, we model each QD with a single level with on-site energy ϵ_ℓ ($\ell = L, R$) and tunnel coupling Ω. In our experiment, Coulomb repulsion allows the occupation of the DQD with only one electron. Dot L is tunnel coupled to an electron source from which electrons may enter at rate Γ_L. Correspondingly, dot R is coupled to a drain with rate Γ_R. The broadening of the current peaks with increasing temperature can be explained by the coupling of the DQD dipole moment to a bosonic heat bath [33,34,44] with ohmic spectral density and a dimensionless coupling strength α [32].

In QDs, spin flips may be caused by various mechanisms such as a hyperfine interaction [5], spin-flip cotunneling [6,7], and spin-orbit interaction [10] with their characteristic dependencies of the decay rates on the Zeeman splitting. In turn, measurements of the spin-flip rates hint at the dominating mechanism. In the present case, the mechanism must explain not only the observed increase of the rate with the Zeeman splitting, but also the significant temperature dependence and the asymmetry between decay and thermal excitation. These requirements can be fulfilled by spin-flip cotunneling [6,7] induced by the spin-conserving tunnel Hamiltonian $H_T = \sum_{k\sigma} t_k(c^\dagger_{k\sigma} d_\sigma + d^\dagger_\sigma c_{k\sigma})$, where the fermionic operators $c_{k\sigma}$ and d_σ annihilate an electron with spin σ in the left lead and the left dot, respectively (spin flips in the right dot do not play a role and will be ignored). In a T-matrix formulation, the impact of H_T is given by an effective coupling that obeys the recursive relation $T = H_T + H_T G_0(E_i)T$, where $G_0(z) = (z - H_0)^{-1}$ is the Green's function in the absence of tunneling and E_i the energy of the initial state [45].

Our focus lies on spin flips in a singly occupied QD, where Coulomb repulsion and the Pauli principle forbid resonant dot-lead tunneling. Then the leading contribution to T is the second-order term $H_T G_0 H_T$ which causes the process schematically shown in Fig. 3(a), where the virtually populated dot states are the empty dot and the singlet state. A spin-up electron flips to the lower Zeeman level, while a lead electron at the Fermi surface is excited and flips. The opposite process requires the decay of a lead electron, which is possible only at sufficiently high temperature. In the Supplemental Material [46], we show that the T matrix can be approximated as $T = \hbar(\sigma^\dagger_\uparrow \sigma_\downarrow \zeta + \sigma^\dagger_\downarrow \sigma_\uparrow \zeta^\dagger)$, where ζ describes quantum noise stemming from electron excitations under spin flip at the Fermi surface of the lead. For the numerical treatment, we employ a Bloch-Redfield master equation [48,49]. The dissipative kernel stemming from T is fully specified by the noise correlation $C(t) = \langle \zeta(0)\zeta^\dagger(t)\rangle$ which in frequency space reads $C(\omega) = \pi\alpha_{\rm spin}\omega n_{\rm th}(\hbar\omega)$ with the Bose function $n_{\rm th}(E) = [\exp(E/kT) - 1]^{-1}$. The dimensionless spin dissipation $\alpha_{\rm spin}$ is our central quantity of interest, because it allows predictions for the spin coherence [50,51]. While $\alpha_{\rm spin}$ can be roughly estimated from the dot-lead coupling Γ_L, the on-site interaction, and the chemical potential [46], we will determine its precise value by fitting our experimental data.

The current peak at $B = 0$ is shown in Fig. 3(b). Proceeding as in Ref. [32], we find the dot-lead rate $\Gamma_R = 5\,\mu$eV, the interdot tunneling $\Omega = 0.85\,\mu$eV, and the dimensionless dissipation strength $\alpha = 0.005$. Due to the asymmetric coupling, $\Gamma_R \ll \Gamma_L$ while Γ_L does not greatly influence the current. In comparison to the dots studied in Ref. [31], Ω is two orders of magnitude smaller and even in comparison to Ref. [32] it is a factor of 2–5 smaller, indicating a very weak interdot coupling in the work here.

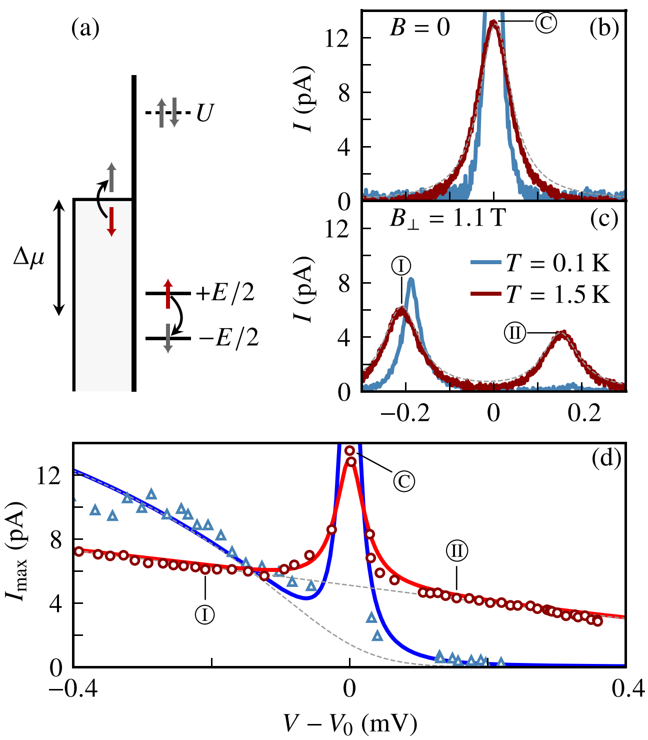

FIG. 3. (a) Spin dissipation due to cotunneling. (b), (c) Measured tunneling current as a function of the bias voltage in the absence ($B = 0$) and presence ($B_\perp = 1.1$ T) of a magnetic field, respectively, for temperatures $T = 100$ mK and $T = 1.5$ K. The resonance peaks are centered around the peak position V_0 at $B = 0$. The dashed line indicates the numerical data for the higher temperature with $\Omega = 0.85\,\mu$eV, $\Gamma_R = 5\,\mu$eV, $\alpha = 0.005$, $\alpha_{\rm spin} = 1.2 \times 10^{-4}$, and $g_L = 0.7$. (d) Corresponding peak heights as a function of the bias voltage. Symbols mark experimental values, while solid and dotted lines indicate numerical data and the analytical approximation in Eq. (1), respectively.

To analyze the spin flips, we focus on the changes with the magnetic field. Figure 3(c) shows the two peaks for $B_\perp = 1.1$ T and two different temperatures. Figure 3(d) shows the height of the peaks as a function of their position for the two different temperatures, where peak II vanishes for higher magnetic fields. In the Supplemental Material [46] we show that also for the parallel magnetic field direction similar results are obtained. Solving numerically our model leads to two fitting parameters in addition to the parameters extracted for $B = 0$ and in addition to Δg extracted from the observed Zeeman splitting, namely the dimensionless spin dissipation $\alpha_{\rm spin} = 1.2 \times 10^{-4}$ and the gyromagnetic ratio of the left dot, $g_L = 0.7$ (for $B_\parallel$ we obtain $g_L = 1$). The experimental results are well reproduced by our model (solid lines) in using these two fitting parameters for both temperatures. At $T = 1.5$ K the theory describes the experimental results. almost perfectly showing that our model is well justified. At $T = 0.1$ K, especially at more negative voltages (higher magnetic fields), deviations between theory and experiment are observed. These deviations might be caused by the influence

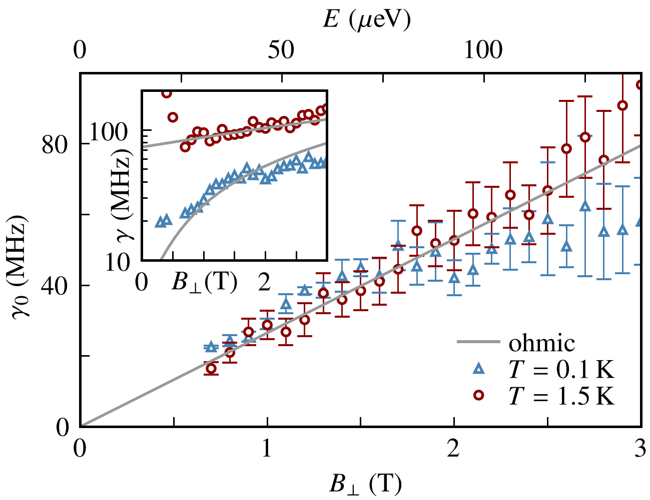

FIG. 4. Spin-flip rate in the zero-temperature limit, γ_0, as a function of the Zeeman splitting (upper axis) and the corresponding magnetic field. The values are obtained from Eq. (1) together with the detailed-balance relation. For the size of the error bars, see the Supplemental Material [46]. Inset: Spin-flip rate $\gamma(E)$ at finite temperature.

of noise on the very sharp peaks [46]. The good agreement for both temperatures clearly hints towards spin-flip cotunneling as the main process.

Energy dependence of the spin decay. We now aim at a more direct access to the spin-flip rate as a function of the Zeeman spitting. We capture the scenario of the spin blockade by a rate equation which holds for sufficiently large magnetic fields such that the two peaks are well separated. We assume that an electron with arbitrary spin orientation enters from the source to the left dot, where it undergoes spin flips with the spin decay rate γ and the thermal excitation rate $\bar{\gamma}$ which are assumed to be linked by the detailed balance relation $\bar{\gamma}(E)/\gamma(E) = \exp(-E/kT)$. At the peak, one Zeeman level is in resonance with the corresponding level of the right dot. The resulting rate equation provides the current [46]

$$I(B) = \frac{2\gamma I_0}{I_0/e + 2\gamma + 2\bar{\gamma}}, \qquad (1)$$

with I_0 the peak height at zero magnetic field and the Zeeman splitting in the left dot, $E = g_L\mu_B B$. Interestingly, for sufficiently large g_L, this result depends on Ω and Γ_R only via I_0.

Equation (1) together with the detailed balance relation provides γ as a function of the Zeeman splitting E and I_0. At low temperatures, the result corresponds to the spontaneous decay rate. Under the assumption that the induced decay is proportional to the thermal occupation of the resonant environmental modes, $n_{\text{th}}(E)$, we may compute the spontaneous decay rate γ_0 also from measurements at higher temperatures. Therefore, we conjecture that $\gamma_0(E) \equiv \gamma(E)/[1 + n_{\text{th}}(E)]$ is temperature independent and grows linearly with the Zeeman splitting. Figure 4 shows the accordingly evaluated experimental data. They exhibit good agreement for $B_\perp \gtrsim 0.5\,\text{T}$, while below this value, the peaks overlap such that Eq. (1) does not hold. Especially for $T = 1.5\,\text{K}$ the agreement is quite good. One obtains spin relaxation rates varying between 20 MHz at 0.7 T and about 80 MHz at 3 T. This linear behavior is directly related to the ohmic spectral density and supports our conjecture of spin-flip cotunneling resolving the current blockade. At $T = 100\,\text{mK}$, one witnesses a deviation which we attribute to the already mentioned underestimation of the peak height. Moreover, for large Zeeman splittings, the thermal excitation rate becomes small, which augments the relative error.

In principle, one may consider other spin-dissipation mechanisms such as spin-orbit or hyperfine interactions. These, however, are expected to show a stronger dependence on the magnetic field and can be ruled out. A further conceivable mechanism to resolve the blockade is dissipative transitions from the left to the right dot [32]. As such transitions occur also when both Zeeman levels are misaligned, they cannot explain the emergence of sharp resonance peaks with the observed asymmetry.

Conclusions. We have used here a spin-dependent blockade mechanism for single electrons in self-assembled DQDs to extract spin relaxation rates directly from the measured resonant tunnel currents. An analysis based on a rate equation provided the spin-flip rates which turned out to grow linearly with the Zeeman splitting. Quantitatively, the spontaneous spin decay rate at 2 T is of the order 50 MHz. Hence, we expect coherence times of roughly 20 ns which corresponds to a few hundred coherent oscillations. The findings here discussed identify spin-flip cotunneling as the dominating decoherence mechanism.

Acknowledgment. This work was supported by the Deutsche Forschungsgemeinschaft (DFG, German Research Foundation) under Germany's Excellence Strategy – EXC 2123 QuantumFrontiers – 390837967, the State of Lower Saxony of Germany via the Hannover School for Nanotechnology, and by the Spanish Ministry of Science, Innovation, and Universities (Grant No. PID2020-117787GB-I00), and by the CSIC Research Platform on Quantum Technologies PTI-001.

[1] D. Loss and D. P. DiVincenzo, Quantum computation with quantum dots, Phys. Rev. A **57**, 120 (1998).

[2] A. J. Weinstein, M. D. Reed, A. M. Jones, R. W. Andrews, D. Barnes, J. Z. Blumoff, L. E. Euliss, K. Eng, B. H. Fong, S. D. Ha, D. R. Hulbert, C. A. C. Jackson, M. Jura, T. E. Keating, J. Kerckhoff, A. A. Kiselev, J. Matten, G. Sabbir, A. Smith, J. Wright *et al.*, Universal logic with encoded spin qubits in silicon, Nature (London) **615**, 817 (2023).

[3] W. Gilbert, T. Tanttu, W. H. Lim, M. Feng, J. Y. Huang, J. D. Cifuentes, S. Serrano, P. Y. Mai, R. C. C. Leon, C. C. Escott, K. M. Itoh, N. V. Abrosimov, H.-J. Pohl, M. L. W. Thewalt, F. E. Hudson, A. Morello, A. Laucht, C. H. Yang, A. Saraiva, and A. S. Dzurak, On-demand electrical control of spin qubits, Nat. Nanotechnol. **18**, 131 (2023).

[4] G. Burkard, T. D. Ladd, A. Pan, J. M. Nichol, and J. R. Petta, Semiconductor spin qubits, Rev. Mod. Phys. **95**, 025003 (2023).

[5] J. Schliemann, A. V. Khaetskii, and D. Loss, Spin decay and quantum parallelism, Phys. Rev. B **66**, 245303 (2002).

[6] F. Qassemi, W. A. Coish, and F. K. Wilhelm, Stationary and transient leakage current in the Pauli spin blockade, Phys. Rev. Lett. **102**, 176806 (2009).

[7] W. A. Coish and F. Qassemi, Leakage-current line shapes from inelastic cotunneling in the Pauli spin blockade regime, Phys. Rev. B **84**, 245407 (2011).

[8] W. A. Coish, J. Fischer, and D. Loss, Exponential decay in a spin bath, Phys. Rev. B **77**, 125329 (2008).

[9] W. A. Coish and D. Loss, Hyperfine interaction in a quantum dot: Non-Markovian electron spin dynamics, Phys. Rev. B **70**, 195340 (2004).

[10] J. Danon and Y. V. Nazarov, Pauli spin blockade in the presence of strong spin-orbit coupling, Phys. Rev. B **80**, 041301(R) (2009).

[11] J.-Y. Wang, G.-Y. Huang, S. Huang, J. Xue, D. Pan, J. Zhao, and H. Xu, Anisotropic Pauli spin-blockade effect and spin-orbit interaction field in an InAs nanowire double quantum dot, Nano Lett. **18**, 4741 (2018).

[12] R. Hanson, B. Witkamp, L. M. K. Vandersypen, L. H. Willems van Beveren, J. M. Elzerman, and L. P. Kouwenhoven, Zeeman energy and spin relaxation in a one-electron quantum dot, Phys. Rev. Lett. **91**, 196802 (2003).

[13] J. M. Elzerman, R. Hanson, L. H. W. v. Beveren, B. Witkamp, L. M. K. Vandersypen, and L. P. Kouwenhoven, Single-shot read-out of an individual electron spin in a quantum dot, Nature (London) **430**, 431 (2004).

[14] S. Amasha, K. MacLean, I. P. Radu, D. M. Zumbühl, M. A. Kastner, M. P. Hanson, and A. C. Gossard, Electrical control of spin relaxation in a quantum dot, Phys. Rev. Lett. **100**, 046803 (2008).

[15] L. C. Camenzind, L. Yu, P. Stano, J. D. Zimmermann, A. C. Gossard, D. Loss, and D. M. Zumbühl, Hyperfine-phonon spin relaxation in a single-electron GaAs quantum dot, Nat. Commun. **9**, 3454 (2018).

[16] A. Kurzmann, P. Stegmann, J. Kerski, R. Schott, A. Ludwig, A. D. Wieck, J. König, A. Lorke, and M. Geller, Optical detection of single-electron tunneling into a semiconductor quantum dot, Phys. Rev. Lett. **122**, 247403 (2019).

[17] L. Banszerus, K. Hecker, S. Möller, E. Icking, K. Watanabe, T. Taniguchi, C. Volk, and C. Stampfer, Spin relaxation in a single-electron graphene quantum dot, Nat. Commun. **13**, 3637 (2022).

[18] K. Ono, D. G. Austing, Y. Tokura, and S. Tarucha, Current rectification by Pauli exclusion in a weakly coupled double quantum dot system, Science **297**, 1313 (2002).

[19] A. C. Johnson, J. R. Petta, J. M. Taylor, A. Yacoby, M. D. Lukin, C. M. Marcus, M. P. Hanson, and A. C. Gossard, Triplet-singlet spin relaxation via nuclei in a double quantum dot, Nature (London) **435**, 925 (2005).

[20] F. H. L. Koppens, K. C. Nowack, and L. M. K. Vandersypen, Spin echo of a single electron spin in a quantum dot, Phys. Rev. Lett. **100**, 236802 (2008).

[21] H. Bluhm, S. Foletti, I. Neder, M. Rudner, D. Mahalu, V. Umansky, and A. Yacoby, Dephasing time of GaAs electron-spin qubits coupled to a nuclear bath exceeding 200 μs, Nat. Phys. **7**, 109 (2011).

[22] V. Srinivasa, K. C. Nowack, M. Shafiei, L. M. K. Vandersypen, and J. M. Taylor, Simultaneous spin-charge relaxation in double quantum dots, Phys. Rev. Lett. **110**, 196803 (2013).

[23] V. F. Maisi, A. Hofmann, M. Röösli, J. Basset, C. Reichl, W. Wegscheider, T. Ihn, and K. Ensslin, Spin-orbit coupling at the level of a single electron, Phys. Rev. Lett. **116**, 136803 (2016).

[24] S. Nadj-Perge, S. M. Frolov, E. P. A. M. Bakkers, and L. P. Kouwenhoven, Spin-orbit qubit in a semiconductor nanowire, Nature (London) **468**, 1084 (2010).

[25] M. D. Schroer, K. D. Petersson, M. Jung, and J. R. Petta, Field tuning the *g* factor in InAs nanowire double quantum dots, Phys. Rev. Lett. **107**, 176811 (2011).

[26] N. S. Lai, W. H. Lim, C. H. Yang, F. A. Zwanenburg, W. A. Coish, F. Qassemi, A. Morello, and A. S. Dzurak, Pauli spin blockade in a highly tunable silicon double quantum dot, Sci. Rep. **1**, 110 (2011).

[27] G. Yamahata, T. Kodera, H. O. H. Churchill, K. Uchida, C. M. Marcus, and S. Oda, Magnetic field dependence of Pauli spin blockade: A window into the sources of spin relaxation in silicon quantum dots, Phys. Rev. B **86**, 115322 (2012).

[28] R. Li, F. E. Hudson, A. S. Dzurak, and A. R. Hamilton, Pauli spin blockade of heavy holes in a silicon double quantum dot, Nano Lett. **15**, 7314 (2015).

[29] M. Brauns, J. Ridderbos, A. Li, E. P. A. M. Bakkers, W. G. van der Wiel, and F. A. Zwanenburg, Anisotropic pauli spin blockade in hole quantum dots, Phys. Rev. B **94**, 041411(R) (2016).

[30] T. Zhang, H. Liu, F. Gao, G. Xu, K. Wang, X. Zhang, G. Cao, T. Wang, J. Zhang, X. Hu, H.-O. Li, and P. Guo, Anisotropic *g*-factor and spin-orbit field in a germanium hut wire double quantum dot, Nano Lett. **21**, 3835 (2021).

[31] S. M. Huang, Y. Tokura, H. Akimoto, K. Kono, J. J. Lin, S. Tarucha, and K. Ono, Spin bottleneck in resonant tunneling through double quantum dots with different Zeeman splittings, Phys. Rev. Lett. **104**, 136801 (2010).

[32] O. Dani, R. Hussein, J. C. Bayer, S. Kohler, and R. J. Haug, Temperature-dependent broadening of coherent current peaks in InAs double quantum dots, Commun. Phys. **5**, 292 (2022).

[33] A. J. Leggett, S. Chakravarty, A. T. Dorsey, M. P. A. Fisher, A. Garg, and W. Zwerger, Dynamics of the dissipative two-state system, Rev. Mod. Phys. **59**, 1 (1987).

[34] P. Hänggi, P. Talkner, and M. Borkovec, Reaction-rate theory: Fifty years after Kramers, Rev. Mod. Phys. **62**, 251 (1990).

[35] Q. Xie, A. Madhukar, P. Chen, and N. P. Kobayashi, Vertically self-organized InAs quantum box islands on GaAs(100), Phys. Rev. Lett. **75**, 2542 (1995).

[36] H. Eisele, O. Flebbe, T. Kalka, C. Preinesberger, F. Heinrichsdorff, A. Krost, D. Bimberg, and M. Dähne-Prietsch, Cross-sectional scanning-tunneling microscopy of stacked InAs quantum dots, Appl. Phys. Lett. **75**, 106 (1999).

[37] P. Barthold, F. Hohls, N. Maire, K. Pierz, and R. J. Haug, Enhanced shot noise in tunneling through a stack of coupled quantum dots, Phys. Rev. Lett. **96**, 246804 (2006).

[38] G. Kießlich, E. Schöll, T. Brandes, F. Hohls, and R. J. Haug, Noise enhancement due to quantum coherence in coupled quantum dots, Phys. Rev. Lett. **99**, 206602 (2007).

[39] M. T. Björk, A. Fuhrer, A. E. Hansen, M. W. Larsson, L. E. Fröberg, and L. Samuelson, Tunable effective *g* factor in InAs nanowire quantum dots, Phys. Rev. B **72**, 201307(R) (2005).

[40] I. Hapke-Wurst, U. Zeitler, R. J. Haug, and K. Pierz, Mapping the *g*-factor anisotropy of InAs self-assembled quantum dots, Physica E **12**, 802 (2002).

[41] J. M. Meyer, I. Hapke-Wurst, U. Zeitler, R. J. Haug, and K. Pierz, Resonant tunneling through InAs quantum dots in tilted magnetic fields: Experimental determination of the *g*-factor anisotropy, Phys. Status Solidi B **224**, 685 (2001).

[42] A. Schwan, B.-M. Meiners, A. Greilich, D. R. Yakovlev, M. Bayer, A. D. B. Maia, A. A. Quivy, and A. B. Henriques, Anisotropy of electron and hole *g*-factors in (In,Ga)As quantum dots, Appl. Phys. Lett. **99**, 221914 (2011).

[43] V. V. Belykh, D. R. Yakovlev, J. J. Schindler, E. A. Zhukov, M. A. Semina, M. Yacob, J. P. Reithmaier, M. Benyoucef, and M. Bayer, Large anisotropy of electron and hole *g*-factors in infrared-emitting InAs/InAlGaAs self-assembled quantum dots, Phys. Rev. B **93**, 125302 (2016).

[44] U. Weiss, *Quantum Dissipative Systems*, 4th ed. (World Scientific, Singapore, 2012).

[45] H. Bruus and K. Flensberg, *Many-Body Quantum Theory in Condensed Matter Physics* (Oxford University Press, New York, 2004).

[46] See Supplemental Material at http://link.aps.org/supplemental/10.1103/PhysRevB.109.L121404 for additional data, data analysis, and the derivation of Eq. (1), which includes Ref. [47].

[47] A. Savitzky and M. J. E. Golay, Smoothing and differentiation of data by simplified least squares procedures, Anal. Chem. **36**, 1627 (1964).

[48] A. G. Redfield, On the theory of relaxation processes, IBM J. Res. Develop. **1**, 19 (1957).

[49] K. Blum, *Density Matrix Theory and Applications*, 2nd ed. (Springer, New York, 1996).

[50] U. Weiss and M. Wollensak, Dynamics of the biased two-level system in metals, Phys. Rev. Lett. **62**, 1663 (1989).

[51] Y. Makhlin, G. Schön, and A. Shnirman, Quantum-state engineering with Josephson-junction devices, Rev. Mod. Phys. **73**, 357 (2001).